Desalination and Water Treatment
www.deswater.com
doi: 10.1080/19443994.2013.768750

51 (2013) 5260–5267
July

Taylor & Francis
Taylor & Francis Group

Optimum operating conditions in hybrid water treatment process of multi-channel ceramic MF and polyethersulfone beads loaded with photocatalyst

Bolor Amarsanaa[a], Jin Yong Park[a,*], Alberto Figoli[b], Enrico Drioli[b]

[a]*Dept. of Environmental Sciences & Biotechnology, Hallym University, Gangwon 200-702, Korea*
Tel. +82 33 248 2152; Fax: +82 33 256 3420; email: jypark@hallym.ac.kr
[b]*Institute on Membrane Technology, ITM-CNR, Via P. Bucci, 87030 Rende, Italy*

Received 15 June 2012; Accepted 24 September 2012

ABSTRACT

The effects of water back-flushing period (FT) and polyethersulfone (PES) beads concentration loaded with titanium dioxide (TiO_2) photocatalyst were investigated in a hybrid process of multi-channel ceramic MF and photocatalyst. The space between the outside of the membrane (0.4 μm pore size) and the module inside was filled with the PES beads. UV at a wavelength of 352 nm was radiated from outside of the acryl module. A quantity of humic acid and kaolin was dissolved in distilled water and utilized here as synthetic water. As a result of FT effect, resistance of membrane fouling (R_f) was decreased when FT decreased from NBF (no back-flushing) to 2 min at BT 10 s. Therefore, the FT 2 min at BT 10 s was the optimal condition to reduce membrane fouling and to maintain high permeate flux in our hybrid process. As a result of photocatalyst PES beads concentration, R_f was minimum at 40 mg/L when photocatalyst beads concentration was changed from 50 to 5 mg/L. The highest treatment efficiency of turbidity was 97.6% at 30 g/L. However, the treatment efficiency of UV_{254} absorbance, which was the organic matter concentration, decreased from 83.5 to 77.3% when PES beads concentration was changed from 50 to 5 mg/L.

Keywords: Microfiltration; Photocatalyst; Hybrid process; Ceramic membrane; Water treatment

1. Introduction

Photocatalytic oxidation, a new type of water pollution control technology, with the characteristics of high efficiency, low-energy consumption and a wide range of application, can oxidize most organic compounds, especially non-biodegradable organic contaminants, by mineralizing them to small inorganic molecules. For this reason, photocatalytic oxidation technology has broad prospects for application. Among various semiconductor photocatalysts, there is a general consensus among researchers that TiO_2 is more superior because of its high activity, large stability to light illumination, and low price [1–4]. In photocatalytic degradation, two modes of TiO_2 application are adopted: (1) TiO_2 immobilized on support materials and (2) TiO_2 suspended in aqueous medium [5,6].

---

*Corresponding author.

7th Aseanian Membrane Society Conference (AMS7), 4–7 July 2012, Busan, Korea

Application of TiO_2 in suspension instead of immobilizing the TiO_2 on solid carriers has shown an improvement in organic degradation efficiencies due to the uniform distribution and large specific surface area. However, classical solid-liquid separation processes, such as sedimentation, centrifugation and coagulation used for separation of the fine TiO_2 particles (typically less than 1 μm), are not effective [7]. In addition to the low reutilization rate, there is also a chance of secondary pollution caused by fine TiO_2 particles in the effluent. Therefore, the recovery of the photocatalysts is one of the main concerns that affect its engineering application on a large scale. A lot of investigations have been conducted aiming at solving this problem [8–12].

In recent years, titanium microsphere has also been proposed as a means to recover TiO_2 photocatalyst. Generally, the core-shell-structured TiO_2 microspheres with a mesoporous surface made of nano-TiO_2 have low density, high specific surface area, and large size favorable for separation [13–16]. But the preparation method and operating conditions have great effect on particle morphology associated with photocatalysis, and many problems existing in the current preparation methods need to be solved by optimizing the process conditions or developing new ones [17].

Membrane separation process for separation and purification has been developed rapidly during the past few decades. It can simultaneously separate and concentrate all pollutants in water by the retention of its microspores without secondary pollution and phase change. In addition, with the advantage of low-energy consumption, its equipments are compact, easy to operate, and capable of continuous operation at room temperature [18]. However, membrane fouling due to the adsorption-precipitation of organic and inorganic compounds onto membranes leads to a decrease in the permeate flux, an increase in membrane cleaning costs and a reduction in the life of the membrane. Although considerable progress has been made in membrane fouling [19,20], techniques for controlling membrane fouling remain inadequate, which is the major obstacle in the successful implementation of membrane separation technology. The TiO_2 photocatalysis-membrane separation coupling technology emerged recently can solve the two problems afore mentioned effectively [21]. The coupling technology not only keeps the characteristics and capacity of the two technologies, but also produces some synergistic effects to overcome the drawbacks of the single technology. On the one hand, the pollutants are oxidized by the photocatalysis, and the selected membranes show the capability not only to retain the photocatalyst, but also to reject partially organic species by controlling the residence time in the reacting system. In other words, the membrane is also a selective barrier for the molecules to be degraded, and thus, the coupling technology could enhance the photocatalytic efficiency and achieve excellent effluent quality. On the other hand, the coupling of photocatalysis and membrane separation could solve or alleviate the problem of flux decline associated with membrane fouling [22].

In this study, the effects of water back-flushing time (FT) and polyethersulfone (PES) beads concentration loaded with titanium dioxide (TiO_2) photocatalyst were investigated in the hybrid process of multi-channel ceramic MF and photocatalyst, and we tried to find their optimal operating conditions.

2. Experiments

2.1. Materials

The multi-channel ceramic MF membrane (HC04) used in the study was coated with α-alumina on a supporting layer of α-alumina, and its pore size was 0.4 μm. We purchased the membrane from Dongseo Inc. in Korea, and the specifications of the multi-channel ceramic membrane are shown in Table 1.

The photocatalyst used was 1.4–1.8 mm polyethersulfone (PES) beads loaded with TiO_2 powder made by Figoli et al. [23,24], which is shown in Table 2. Instead of natural organic matters and fine inorganic particles in natural water source, a quantity of humic acid and kaolin was dissolved in distilled water. It was then used as synthetic water in our experiment. UV with 352 nm was radiated from outside of the acryl module by 2 UV lamps (F8T5BLB, Sankyo, Japan) as shown in Table 3.

Table 1
Specifications of the multi-channel ceramic microfiltration (HC04) used in this study

Membrane	HC04
Pore size (μm)	0.4
No. of channels	7
Outer diameter (mm)	20
Inner diameter (mm)	4
Length (mm)	235
Surface area (cm^2)	206.7
Material	α-alumina coating on α-alumina support
Company	Dongseo Inc. in Republic of Korea

Table 2
Specification of the TiO_2-loaded beads employed in this study

Material of the beads	Polyethersulfone (PES)
TiO_2 coating method	Phase inversion
Diameter (mm)	1.4–1.8
Weight (mg)	1.3–1.8
Average weight (mg)	1.5

Table 3
Specification of UV Lamp employed in this study

Wavelength (nm)	352
Power (W)	8
Model number	F8T5BLB
Company	Sankyo (Japan)

2.2. Hybrid membrane module

To be able to remove the turbidity and NOM, the hybrid module was constructed by packing PES beads loaded with TiO_2 powder between the module inside and outside of a ceramic membrane. In addition, 100 meshes (0.150 mm), which was extremely smaller than 1.4–1.8 mm particle size of the photocatalyst beads used here, were installed at the outlet of the hybrid module to prevent PES beads loss into the treated water tank.

2.3. Experimental procedure

The advanced water treatment system using a hybrid module (6) of multi-channel ceramic microfiltration and photocatalyst adsorption is shown in Fig. 1, which was used at our previous study [25]. We performed cross-flow filtration for the multi-channel ceramic membrane and periodic water back-flushing using permeated water. The hybrid module (6) filled with 40 g/L of PES beads was installed in the advanced water treatment system. Then, the feed tank (1) was filled with 10 L of prepared synthetic water composed of humic acid and kaolin, and the temperature of the feed water was constantly maintained by using a constant temperature circulator (3) (Model 1146, VWR, USA). Also, the synthetic feed water was continuously mixed by a stirrer (4) to maintain the homogeneous condition of the feed water, and it was caused to flow into the inside of the multi-channel ceramic membrane by a pump (2) (Procon, Standex Co., USA). The feed flow rate was measured by a flowmeter (5) (NP-127, Tokyo Keiso, Japan). The flow rate and pressure of the feed water that flowed into the hybrid module was constantly maintained by controlling valves (9) of both the bypass pipe of the pump (2) and the concentrate pipe. The permeate flux treated by both the multi-channel ceramic membrane and photocatalyst was measured by an electric balance (11) (Ohaus, USA). The permeate water flowed into the back-washing tank (13) if the permeate flux had not been measured. After the treated water was over a

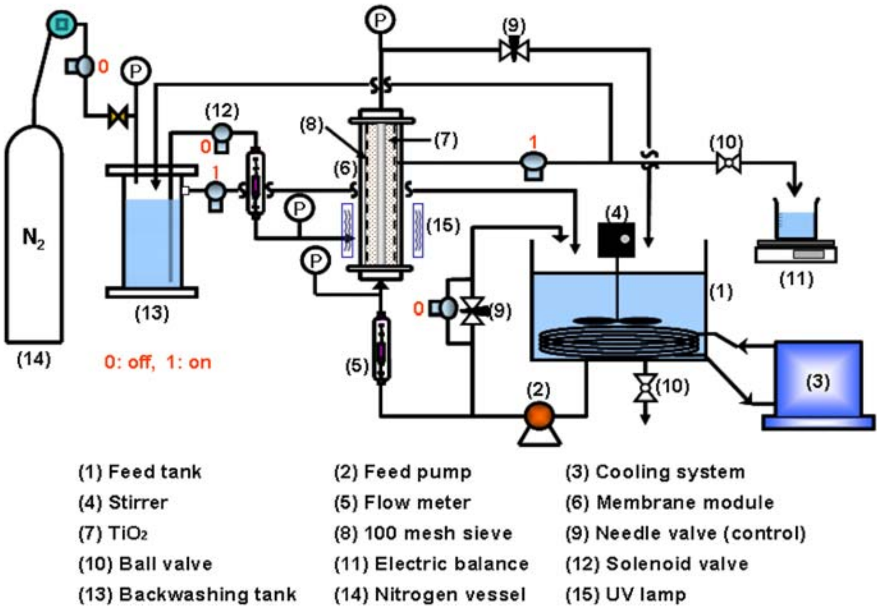

Fig. 1. Apparatus of advanced water treatment system using hybrid module of ceramic microfiltration and PES beads loaded with TiO_2 with periodic water back-flushing [25].

certain level in the back-washing tank (13), it was recycled to the feed tank (1) to maintain a constant concentration of the feed water during operation.

Kaolin was fixed at 30 mg/L, and humic acid was also fixed as 6 and 10 mg/L in the synthetic feed water to study the effect of water back-flushing condition and the photocatalyst beads concentration. The back-flushing time (BT) was fixed at 10 s, and filtration time (FT) was changed as 2, 4, 6, 8, and 10 min to see effect of back-flushing period. Also, the photocatalyst beads concentration was varied at 5, 10, 20, 30, 40, and 50 g/L in the experiment of effect of photocatalyst concentration. We observed the permeate flux (*J*) during total filtration time of 180 min under each condition. Under all experimental conditions, the TMP (transmembrane pressure) was maintained at 0.81 bar, the water back-flushing pressure at 1.0 bar, the feed flow rate at 1.0 L/min, and the feed water temperature at 20℃.

The quality of feed water and treated water was analyzed to evaluate the treatment efficiencies of turbid materials and dissolved organic matters. Turbidity was measured by a turbidimeter (2100 N, HACH, USA), and UV_{254} absorbance was analyzed by a UV spectrophotometer (GENESYS 10 UV, Thermo, USA).

3. Results and discussion

The effects of water back-flushing period (FT) and PES beads concentration loaded with TiO_2 photocatalyst were investigated and the optimal operating conditions found in a hybrid process of multi-channel ceramic MF and photocatalyst for advanced treatment water treatment. Resistances of the membrane, boundary layer, and membrane fouling (R_m, R_b, and R_f) were calculated from permeate flux (*J*) data using the resistance-in-series filtration equation as the same method as our previous study [26].

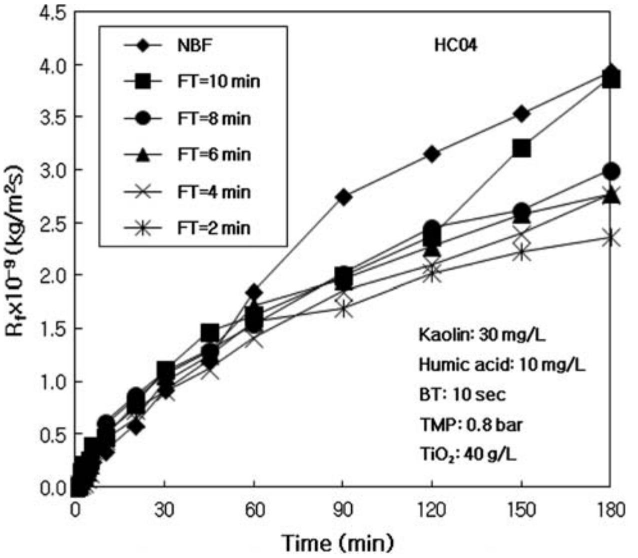

Fig. 2. Effect of water back-flushing period on resistance of membrane fouling in hybrid process of multi-channel ceramic MF and PES beads loaded with TiO_2.

3.1. Effect of water back-flushing period

As plotted in Fig. 2, the result of resistance membrane (R_f) in the experiment of FT effect at fixed 10 s back-flushing time showed the highest R_f value at no back-flushing (NBF) condition. And the R_f value decreased when FT decreased from NBF to 2 min at fixed BT 10 s. This result have the same trend with that of our previous study [25] using a tubular ceramic ultrafiltration membrane with the pore size of 0.05 μm. After 180 min operation, the $R_{f,180}$ value was 2.359×10^9 kg/m^{2}s at 2 min of FT, as arranged in Table 4. This $R_{f,180}$ value should be much smaller than the $R_{f,180}$ value of 3.929×10^9 kg/m^{2}s at NBF. In this study [25], the permeate flux was rapidly decreased, and there was no permeate flux after 60 min' operation

Table 4
Effect of water back-flushing period on filtration factors for hybrid process of multi-channel ceramic MF and PES beads loaded with TiO_2 (BT 10 s)

FT (min)	NBF*	10	8	6	4	2
$R_m \times 10^{-9}$ (kg/m^2 s)	0.800	0.728	0.789	0.764	0.777	0.805
$R_b \times 10^{-9}$ (kg/m^{2}s)	0.077	0.079	0.070	0.089	0.024	0.032
$R_{f,180} \times 10^{-9}$ (kg/m^2 s)	3.929	3.869	2.995	2.771	2.766	2.359
J_0 (L/m^2 h)	322	350	329	331	352	337
J_{180} (L/m^2 h)	59	60	73	78	79	88
J_{180}/J_0	0.182	0.173	0.223	0.235	0.225	0.262
V_T (L)	6.31	6.69	6.70	6.80	7.39	7.41

*No back-flushing.

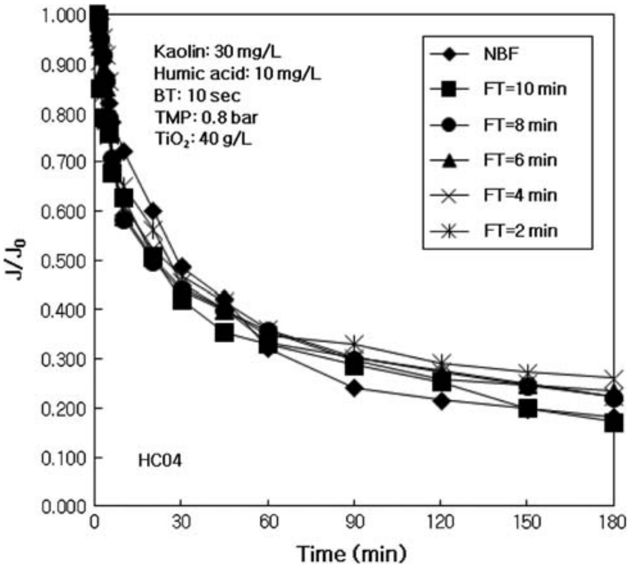

Fig. 3. Effect of water back-flushing period on dimensionless permeate flux in hybrid process of multi-channel ceramic MF and PES beads loaded with TiO_2.

because the UF membrane had the smaller pore than HC04 MF used here, and the membrane fouling was formed the easier. The $R_{f,180}$ was dramatically dropped from 10 to 8 min of FT, but the drop difference of $R_{f,180}$ was not high from 6 to 2 min. It means that FT 2 min at BT 10 s was the optimal condition to reduce membrane fouling in our hybrid process of MF and PES beads loaded with TiO_2. However, the effect of FT on membrane fouling was not high at lower FT than 6 min.

Fig. 3 presented the dimensionless permeate flux (J_{180}/J_0) when FT changed from NBF to 2 min of FT. The J/J_0 value increased when FT changed from NBF to 2 min of FT. As shown in Table 4, the value of J_{180}/J_0 increased from 0.182 to 0.262 from NBF to 2 min of FT, and the highest value of J_{180}/J_0 after 180 min operation could be found at FT 2 min. Also, the maximum value of total permeated volume (V_T) of 7.41 L could be acquired at FT 2 min during 180 min operation in our hybrid system.

As arranged in Table 5, the treatment efficiency of turbidity increased a little from 96.7 to 97.5% when FT decreased from 10 to 2 min and was the maximum value of 97.8% at NBF. But the treatment efficiency of UV_{254} increased much from 80.2 to 88.9% as shown in Table 6. The treatment efficiencies of turbidity and UV_{254} were the highest value at NBF because of the most severe secondary membrane by the highest membrane fouling in our experimental condition. Then, PES beads could be maintained clearer as FT decreased from 10 to 2 min, and photo-oxidation and adsorption by PES beads loaded TiO_2 was the most effective at 2 min of FT. Therefore, the highest efficient condition of our hybrid water treatment system by ceramic MF and photocatalyst was FT 2 min and BT 10 s in the experimental range of this study. The treatment efficiencies of turbidity and UV_{254} in this study have the exactly same trend with those of our previous study [25] using a tubular ceramic ultrafiltration membrane.

3.2. Effect of PES beads concentration

As a result of PES beads concentration effect shown in Fig. 4, the R_f value could maintain the lowest at 40 g/L when PES beads concentration changed from 50 to 5 g/L. And the minimum and the maximum value of R_f after 180 min operation ($R_{f,180}$) were 1.958×10^9 kg/m^{2}s at 40 g/L and 2.701×10^9 kg/m^{2}s

Table 5
Water quality and treatment efficiency of turbidity in the hybrid process of multi-channel ceramic MF and PES beads loaded with TiO_2 for the effect of water back-flushing period (BT 10 s)

Experimental condition			Turbidity (NTU)				Average treatment efficiency (%)
Kaolin (mg/L)	Humic acid (mg/L)	FT (min)	Feed water		Treated water		
			Range	Average	Range	Average	
30	10	NBF*	25.2–31.1	27.9	0.475–0.725	0.618	97.8
		10	30.3–35.0	32.3	0.640–1.300	1.059	96.7
		8	37.5–32.1	29.8	0.622–1.095	0.849	97.1
		6	28.5–33.4	30.6	0.558–1.010	0.838	97.3
		4	24.5–33.1	29.9	0.531–1.000	0.760	97.5
		2	29.8–31.2	30.6	0.578–0.968	0.773	97.5

*No back-flushing.

Table 6
Water quality and treatment efficiency of UV_{254} absorbance in the hybrid process of multi-channel ceramic MF and PES beads loaded with TiO_2 for the effect of water back-flushing period (BT 10 s)

Experimental condition			UV_{254} absorbance (cm^{-1})				Average treatment efficiency (%)
Kaolin (mg/L)	Humic acid (mg/L)	FT (min)	Feed water		Treated water		
			Range	Average	Range	Average	
30	10	NBF*	0.108–0.185	0.143	0.004–0.012	0.008	94.4
		10	0.112–0.191	0.147	0.016–0.048	0.029	80.2
		8	0.111–0.186	0.144	0.009–0.025	0.018	87.8
		6	0.110–0.185	0.138	0.008–0.024	0.017	87.7
		4	0.118–0.180	0.141	0.008–0.023	0.017	88.3
		2	0.122–0.178	0.144	0.010–0.022	0.016	88.9

*No back-flushing.

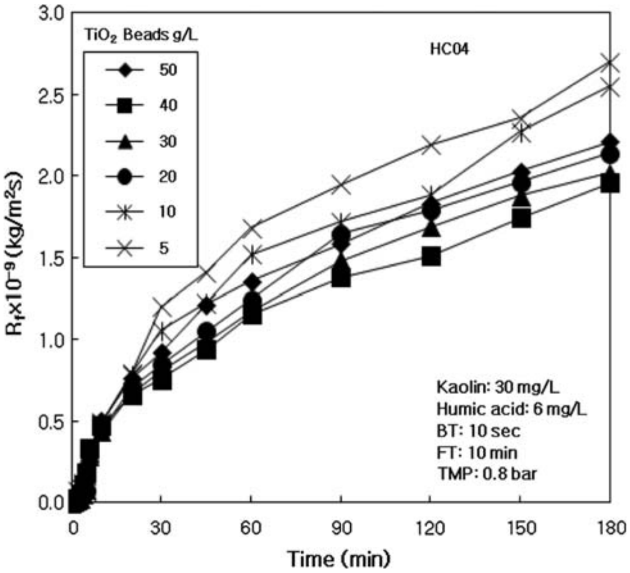

Fig. 4. Effect of PES beads concentration on resistance of membrane fouling in hybrid process of multi-channel ceramic MF and PES beads loaded with TiO_2.

at 5 g/L of PES beads as shown in Table 7, respectively. It means that the 5 g/L of PES beads could be too low and the 40 g/L could be the optimum concentration for the most effective photo-oxidation and adsorption by PES beads to remove pollutants and to reduce the membrane fouling in our experimental range of the hybrid water treatment system. In the previous study [25], the minimum $R_{f,180}$ value was shown at 40 g/L of polypropylene (PP) beads coated with TiO_2 powder by plasma chemical vapor deposition (CVD) method, too.

As shown in Fig. 5, the J/J_0 value could maintain the highest at 40 g/L in our range of PES beads concentration, but the difference of J/J_0 was not large. And the maximum and the minimum value of J/J_0 were 0.312 at 40 g/L and 0.245 at 5 g/L of PES beads in Table 7, respectively. Therefore, the maximum value of V_T of 8.15 L could be acquired at 40 g/L of PES beads during 180 min operation in our hybrid system because the high flux could be maintained at this PES beads concentration.

Table 7
Effect of PES beads concentration on filtration factors for the hybrid process of multi-channel ceramic MF and PES beads loaded with TiO_2

TiO_2 (g/L)	50	40	30	20	10	5
$R_m \times 10^{-9}$ (kg/m^{2}s)	0.810	0.812	0.787	0.799	0.818	0.797
$R_b \times 10^{-9}$ (kg/m^{2}s)	0.026	0.075	0.056	0.057	0.062	0.077
$R_{f,180} \times 10^{-9}$ (kg/m^{2}s)	2.210	1.958	2.017	2.142	2.550	2.701
J_0 (L/m^{2}hr)	338	318	335	330	321	323
J_{180} (L/m^{2}hr)	93	99	99	94	82	79
J_{180}/J_0	0.274	0.312	0.295	0.285	0.257	0.245
V_T (L)	7.69	8.15	8.14	7.82	7.21	6.82

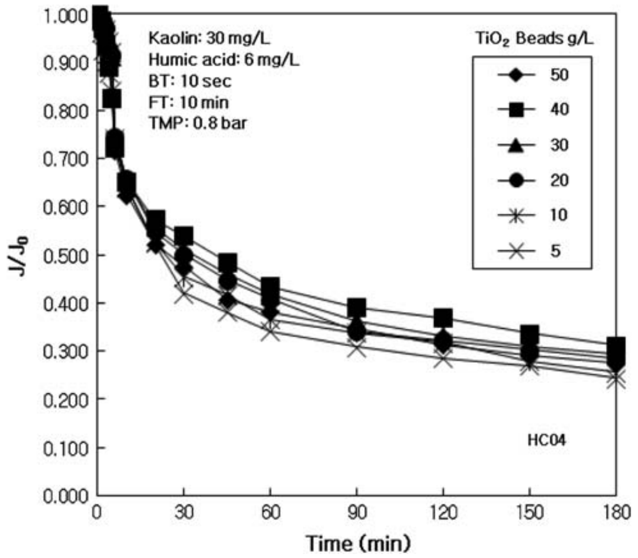

Fig. 5. Effect of PES beads concentration on dimensionless permeate flux in hybrid process of multi-channel ceramic MF and PES beads loaded with TiO_2.

The highest treatment efficiency of turbidity was 97.6% at 30 g/L and the lowest one was 96.5% at 50 g/L of PES beads concentration as shown in Table 8. But the treatment efficiency difference of turbidity was not highly dependent on PES beads concentration. In the previous study [25], the treatment efficiency of turbidity decreased a little from 99.1 to 98.6%, when PP beads concentration was changed from 40 to 10 g/L. However, the treatment efficiency of UV_{254} absorbance, which was the organic matter concentration, decreased from 83.5 to 77.3%, when PES beads concentration was changed from 50 to 5 g/L, as arranged in Table 9. In the previous study [25], the treatment efficiency of UV_{254} absorbance decreased from 96.1 to 92.9% when PP beads concentration was changed from 40 to 10 g/L, too. The treatment efficiency difference of UV_{254} absorbance was not high from 82.6 to 83.5%, when the PES beads concentration was changed from 30 to 50 g/L. Therefore, the optimal PES beads concentration for the highest treatment efficiency should be 30 g/L in this hybrid process of multi-channel ceramic MF and PES beads loaded with TiO_2.

4. Conclusions

In this study, the effect of water back-flushing period and PES beads concentration was observed for finding out the optimum condition in the advanced water treatment by hybrid process of multi-channel ceramic MF and PES beads loaded with TiO_2 photocatalyst. The optimal condition could be FT 2 min at BT 10 s to reduce membrane fouling in our hybrid process. However, the effect of FT on membrane fouling was not high at lower FT than 6 min. The maximum value of total permeated volume could be acquired at FT 2 min during 180 min operation in our hybrid system. The highest efficient condition of our hybrid water treatment system by ceramic MF and photocatalyst was FT 2 min and BT 10 s in the experimental range of this study. The 40 g/L of PES beads could be the optimum concentration for the most effective photo-oxidation and adsorption by PES beads to remove pollutants and to reduce the membrane fouling in our experimental range of the hybrid water treatment system. But the optimal PES beads concentration for the highest treatment efficiency should be 30 g/L in this hybrid process of multi-channel ceramic MF and PES beads loaded with TiO_2.

Table 8
Water quality and treatment efficiency of turbidity in the hybrid process of multi-channel ceramic MF and PES beads loaded with TiO_2 for the effect of PES beads concentration

Experimental condition			Turbidity (NTU)				Average treatment efficiency (%)
Kaolin (mg/L)	Humic acid (mg/L)	TiO_2 (g/L)	Feed water		Treated water		
			Range	Average	Range	Average	
30	6	50	22.1–30.2	25.7	0.742–1.050	0.911	96.5
		40	25.3–30.1	27.6	0.605–0.801	0.696	97.5
		30	23.4–29.8	26.4	0.521–0.723	0.621	97.6
		20	23.2–30.5	26.2	0.595–0.845	0.719	97.3
		10	24.1–29.7	27.1	0.654–0.892	0.794	97.1
		5	24.8–30.2	27.2	0.598–0.897	0.719	97.4

Table 9
Water quality and treatment efficiency of UV_{254} absorbance in the hybrid process of multi-channel ceramic MF and PES beads loaded with TiO_2 for the effect of PES beads concentration

Experimental condition			UV_{254} absorbance (cm^{-1})				Average treatment efficiency (%)
Kaolin (mg/L)	Humic acid (mg/L)	TiO_2 (g/L)	Feed water		Treated water		
			Range	Average	Range	Average	
30	6	50	0.073–0.113	0.087	0.012–0.017	0.014	83.5
		40	0.062–0.112	0.085	0.011–0.018	0.015	82.6
		30	0.063–0.110	0.081	0.010–0.018	0.014	82.6
		20	0.065–0.112	0.084	0.012–0.019	0.016	81.1
		10	0.060–0.118	0.086	0.015–0.022	0.019	78.2
		5	0.068–0.108	0.084	0.012–0.023	0.019	77.3

Acknowledgments

This research was supported by the National Research Foundation of Korea (NRF) grant funded by the Korea government (MEST) (No. 2009-0090428) and by Hallym University Research Fund, 2012 (HRF-201209-019).

References

[1] N. Lydakis-Simantiris, D. Riga, E. Katsivela, D. Mantzavinos, N.P. Xekoukoulotakis, Disinfection of spring water and secondary treated municipal wastewater by TiO_2 photocatalysis, Desalination 250 (2010) 351–355.

[2] J.-M. Herrmann, C. Duchamp, M. Karkmaz, Bui Thu Hoai, H. Lachheb, E. Puzenat, C. Guillard, Environmental green chemistry as defined by photocatalysis, J. Hazard. Mater. 146 (2007) 624–629.

[3] X.H. Wu, P.B. Su, H.L. Liu, L.L. Qi, Photocatalytic degradation of Rhodamine B under visible light with Nd-doped titanium dioxide films, J. Rare Earths 27 (2009) 739–743.

[4] A. Fujishima, X.T. Zhang, Titanium dioxide photocatalysis: Present situation and future approaches, C.R. Chim. 9 (2006) 750–760.

[5] S. Matsuzawa, C. Maneerat, Y. Hayata, T. Hirakawa, N. Negishi, T. Sano, Immobilization of TiO_2 nanoparticles on polymeric substrates by using electrostatic interaction in the aqueous phase, Appl. Catal. B Environ. 83 (2008) 39–45.

[6] R. Molinari, L. Palmisano, E. Drioli, M. Schiavello, Studies on various reactor configurations for coupling photocatalysis and membrane processes in water purification, J. Membr. Sci. 206 (2006) 399–415.

[7] V. Augugliaro, M. Litter, L. Palmisano, J. Soria, The combination of heterogeneous photocatalysis with chemical and physical operations: A tool for improving the photoprocess performance, J. Photochem. Photobiol. C: Photochem. Rev. 7 (2006) 127–144.

[8] R. Pelton, X. Geng, M. Brook, Photocatalytic paper from colloidal TiO_2−fact of fantasy, Adv. Colloid Interf. Sci. 127 (2006) 42–53.

[9] X.Z. Li, H. Liu, L.F. Cheng, H.J. Tong, Photocatalytic oxidation using a new catalyst−TiO_2 icrosphere-for water and wastewater treatment, Environ. Sci. Technol. 37 (2003) 3989–3994.

[10] K. Azrague, E. Puech-Costes, P. Aimar, M.T. Maurette, F. Benoit-Marquie, Membrane photoreactor (MPR) for the mineralisation of organic pollutants from turbid effluents, J. Membr. Sci. 258 (2005) 71−77.

[11] M. Pidou, S.A. Parsons, G. Raymond, P. Jeffery, T. Stephenson, B. Jefferson, Fouling control of a membrane coupled photocatalytic process treating greywater, Water Res. 43 (2009) 3932–3939.

[12] R. Molinari, C. Grande, E. Driloli, L. Palmisano, M. Schiavello, Photocatalytic membrane reactors for degradation of organic pollutants in water, Catal. Today 37 (2001) 273–279.

[13] R.H.S. Jansen, J.W. de Rijk, A. Zwijnenburg, M.H.V. Mulder, M. Wessling, Hollow fiber membrane contactors−A means to study the reaction kinetics of humic substance ozonation, J. Membr. Sci. 257 (2005) 48–59.

[14] K.W. Park, K.H. Choo, M.H. Kim, Use of a combined photocatalysis/ microfiltration system for natural organic matter removal, Membr. J. 14(2) (2004) 149–156.

[15] Y.T. Lee, J.K. Oh, Membrane fouling effect with organic-inorganic materials using the membrane separation in drinking water treatment process, Membr. J. 13(4) (2003) 219–228.

[16] J.H. Xu, W.L. Dai, J. Li, Novel core-shell structured mesoporous titania microspheres: Preparation, characterization and excellent photocatalytic activity in phenol abatement, J. Photochem. Photobiol. A: Chem. 195 (2008) 284–294.

[17] V. Abetz, T. Brinkmann, M. Dijkstra, K. Ebert, D. Fritsch, K. Ohlrogge, Developments in membrane research: from material via process design to industrial application, Adv. Eng. Mater. 8 (2006) 328–358.

[18] F.G. Meng, S.R. Chae, A. Drews, M. Kraume, H.-S. Shind, F. Yang, Recent advances in membrane bioreactors (MBRs): Membrane fouling and membrane material, Water Res. 43 (2009) 1489–1512.

[19] C.X. Liu, D.R. Zhang, Y. He, X.S. Zhaob, R. Bai, Modification of membrane surface for anti-biofouling performance. Effect of anti-adhesion and antibacterial approaches, J. Membr. Sci. 346 (2010) 121–130.

[20] Y. Yoon, R.M. Lueptow, Removal of organic contaminants by RO and NF membranes, J. Membr. Sci. 261 (2005) 76–86.

[21] E. Erdim, E. Soyer, S. Tasiyici, I. Koyuncu, Hybrid photocatalysis/submerged microfiltration membrane system for drinking water treatment, Desalin. Water Treat. 9 (2009) 165–174.

[22] S. Mozia, Photocatalytic membrane reactors (PMRs) in water and wastewater treatment, Sep. Purif. Technol. 73 (2010) 71–91.

[23] A. Figoli, G. De Luca, E. Longavita, E. Drioli, PEEKWC Capsules Prepared by Phase Inversion Technique: A Morphological and Dimensional Study, Sep. Sci. Technol. 42 (2007) 2809–2827.

[24] M.G. Buonomenna, A. Figoli, I. Spezzano, M. Davoli, E. Drioli, New PVDF microcapsules for application in catalysis, Appl. Catal. B: Environ. 80 (2008) 185–194.

[25] S.C. Gao, J.Y. Park, Advanced water treatment of high turbidity source by hybrid process of ceramic ultrafiltration and photocatalyst: 1. Effect of photocatalyst and water-back-flushing condition, Membr. J. 21 (2011) 127–140.

[26] J.Y. Park, S.J. Choi, B.R. Park, Effect of N_2-back-flushing in multi-channels ceramic microfiltration system for paper wastewater treatment, Desalination 202 (2007) 207–214.